iScience, Volume *23*

Supplemental Information

Rapid and Selective Targeting of Heterogeneous Pancreatic Neuroendocrine Tumors

G. Kate Park, Jeong Heon Lee, Eduardo Soriano, Myunghwan Choi, Kai Bao, Wataru Katagiri, Do-Yeon Kim, Ji-Hye Paik, Seok-Hyun Yun, John V. Frangioni, Thomas E. Clancy, Satoshi Kashiwagi, Maged Henary, and Hak Soo Choi

TRANSPARENT METHODS

Chemicals and Methods

All chemicals and solvents were of American Chemical Society grade or HPLC purity and were used as received. HPLC grade acetonitrile (CH_3CN) and water were purchased from VWR International (West Chester, PA) and American Bioanalytic (Natick, MA), respectively. All other chemicals were purchased from Fisher Scientific (Pittsburgh, PA, USA) and Sigma-Aldrich (Saint Louis, MO). Melting points (mp, open Pyrex capillary) were measured on a Meltemp apparatus and are uncorrected. ^{1}H- and ^{13}C-NMR spectra were recorded on a BrukerAvance (400 MHz) spectrometer. Vis/NIR absorption spectra were recorded on a Perkin Elmer Lambda 20 spectrophotometer or Varian 50 scan UV-visible spectrophotometer. Chemical purity was also confirmed using ultra-performance liquid chromatography (UPLC, Waters, Milford, MA) combined with simultaneous evaporative light scattering detection (ELSD), absorbance (photodiode array; PDA), fluorescence, and electrospray time-of-flight (ES-TOF) mass spectrometry (MS).

Synthesis of symmetrical and unsymmetrical phenoxazine derivatives: A series of phenoxazinium based dyes x-x was synthesized through the condensation reaction between a p-nitrosoanilines with substituted naphthalen-1-ols, naphthalen-1-amines or 3-aminophenols in acidic solutions, as shown in Scheme 1. The required precursor, nitrosophenol can be obtained by the usual procedure involving treatment of either di-alkylated or mono alkylated m-aminophenol with sodium nitrite in the presence of hydrochloric acid. Since nitroso reagent constitutes the first half of the dye, the alternate half has to be carefully selected since they determine the substituents present at the 5- and 9- positions of the tetracyclic system and 5- and 7- positions of the tricyclic system of the target compounds. The cyclization occurs in the presence of a strong mineral acid, such as perchloric or hydrochloric acids and is driven by the formation of the aromatic dye.

***N*-(7-(dimethylamino)-3*H*-phenoxazin-3-ylidene)-*N*-methylmethanaminium chloride (Ox61):** A mixture of compound 3 and 5 (2 mmol) in *i*-PrOH (20 mL) was stirred under an inert atmosphere. 2 mol eq of HCl was added, and the mixture was heated under reflux for 6 h. The dark blue solution was concentrated under reduced pressure and the residue was purified by silica gel column chromatography, using acetone/methanol (from 10:1 to 10:2 v/v). The dark blue fractions where concentrated to a total volume of 2 mL, and a 1:1 mixture of EtOAc and Et_2O (20 mL) was added

to crystallize the product. The mixture was ultrasonicated for 10 min and filtered. The powder was washed with EtOAc and Et_2O then dried under reduced pressure. Yield 45%; mp 190 °C; ^{1}H-NMR (400 MHz, MeOD-d4): δ ppm 3.42 (s, 12 H), 6.90 (s, 2 H), 7.37 (d, *J* = 7.07 Hz, 2 H), 7.72 (br. s., 2 H); ^{13}C-NMR (100 MHz, MeOD-d4): δ ppm 40.40, 96.12, 117.18, 133.76, 148.92, 157.90.

***N*-(7-(dimethylamino)-2-methyl-3*H*-phenoxazin-3-ylidene)ethanaminium perchlorate (Ox89):** A mixture of 3-methoxy-*N,N*-dimethyl-4-nitrosoaniline with 2 mol eq of perchloric acid in *i*-PrOH (10 mL) was stirred at 30o C. A solution of compound 3-(Ethylamino)-4-methylphenol in 90% *i*-PrOH (10 mL) was added dropwise to the above mixture during 45 min. The reaction was monitored via UV-Vis. The dark blue solution was evaporated, followed by purification using column chromatography with CH_2Cl_2/MeOH from 10:1 to 1:1 (v/v) and the dark blue solution was evaporated. To a solution of the residue EtOH or MeOH (2 mL), was added AcOEt (20 mL). After ultrasonication for 10 min, the mixture was filtrated. The powder was washed by AcOEt and Et_2O then dried in under reduced pressure. Yield (30%); mp: > 260 °C; ^{1}H-NMR (400 MHz, DMSO-d_6) δ ppm 7.59 (d, *J* = 9.09 Hz, 1 H), 7.42 (br. s., 1 H), 7.21 (d, *J* = 9.09 Hz, 1 H), 6.69 (br. s., 2 H), 3.50 (q, *J* = 5.81 Hz, 2 H), 3.28 (s, 6 H), 2.30 (s,3 H), 1.27 (t, *J* = 12.8, 4 H); ^{13}C-NMR (100 MHz, DMSO-d_6): δ ppm 157.25, 156.44, 148.52, 147.82, 134.19, 133.17, 132.64, 132.21, 129.33, 116.93, 95.96, 93.87, 41.15, 39.02, 17.42, 13.86; HRMS (TOF MS ES$^+$): calcd for $C_{17}H_{20}N_3O^+$: m/z 282.1601 ([M]$^+$), found: m/z 282.1435 [M]$^+$.

***N*-(7-(dimethylamino)-3*H*-phenoxazin-3-ylidene)-*N*-ethylethanaminium perchlorate (Ox261):** The compound was prepared as reported previously with slight modification to method.(Ge et al., 2008) *N'N*-methyl-4-nitrosoaniline was used instead of 3-methoxy-*N,N*-dimethyl-4-nitrosoaniline for the condensation reaction. Yield (11%); mp: > 260 °C; ^{1}H-NMR (400 MHz, Acetone-d_6) δ ppm 7.83-7.85 (m, 2H, Ar-H), 7.48-7.54 (m, 2H, Ar-H), 6.97-7.02 (m, 2H, Ar-H), 3.89-3.84 (m, 4H, CH_2), 3.53 (s, 6H, CH_3), 1.40-1.44 (m, 6H, CH_3); ^{13}C-NMR (100MHz, $CDCl_3$) δ ppm 117.6, 117.4, 96.3, 96.2, 46.5, 40.9, 21.1; HRMS (TOF MS ES$^+$): calcd for $C_{18}H_{22}N_3O^+$: m/z 296.3862 ([M]$^+$), found: m/z 295.5393 [M]$^+$.

***N*-(7-(diethylamino)-3*H*-phenoxazin-3-ylidene)-*N*-ethylethanaminium chloride (Ox96):** The compound was prepared as reported previously.(Ge et al., 2008) Yield 40%; mp: 204 °C (dec.); ^{1}H-

NMR (400 MHz , MeOD-d4) δ ppm 7.81 (d, *J* = 8.8 Hz, 2 H), 7.41 (d, *J* = 8.8 Hz, 2 H), 6.98 (br. s., 2 H), 3.86 - 3.72 (m, 8 H), 1.38 (br. s., 12 H); ^{13}C-NMR (100 MHz, MeOD-d4) δ ppm 157.9, 151.0, 135.7, 118.7, 97.5, 47.8, 13.2; HRMS (TOF MS ES$^+$): calcd for $C_{20}H_{26}N_3O^+$: m/z 324.2070 ([M]$^+$), found: m/z 324.1858 [M]$^+$.

1-(7-(dimethylamino)-3*H*-phenoxazin-3-ylidene)pyrrolidin-1-ium perchlorate (Ox266): The compound was prepared as reported previously with slight modification to method.(Ge et al., 2008) *N'N*-methyl-4-nitrosoaniline was used instead of 3-methoxy-*N,N*-dimethyl-4-nitrosoaniline for the condensation reaction. Yield 5%; mp: > 260 °C; ^{1}H-NMR (400 MHz, DMSO-d_6) **δ** ppm 7.72 (s, 2H, Ar-H), 7.33 (d, *J* = 9.6 Hz, 1H, Ar-H), 7.23 (d, *J* = 9.2 Hz, 1H, Ar-H), 6.86 (s, 1H, Ar-H), 6.73 (s, 1H, Ar-H), 3.66-3.73 (m, 4H, CH_2), 3.33 (s, 6H, CH_3), 2.06 (s, 4H, CH_2); ^{13}C-NMR (100MHz, $CDCl_3$) **δ** ppm 157.3, 154.9, 148.8, 148.6, 134.6, 134.3, 133.9, 133.5, 119.2, 117.5, 97.2, 96.7, 50.4, 50.1, 41.6 25.2, 24.9; HRMS (TOF MS ES$^+$): calcd for $C_{18}H_{20}N_3O^+$: m/z 294.1601 ([M]$^+$), found: m/z 294.1310 [M]$^+$.

1-(7-(dimethylamino)-3*H*-phenoxazin-3-ylidene)piperidin-1-ium perchlorate (Ox269): The compound was prepared as reported previously with slight modification to method.(Ge et al., 2008) *N'N*-methyl-4-nitrosoaniline was used instead of 3-methoxy-*N,N*-dimethyl-4-nitrosoaniline for the condensation reaction. Yield (15%); m.p 255-257 °C; ^{1}H-NMR (400 MHz, DMSO-d_6) δ 7.76-7.80 (s, 2H, Ar-H), 7.58-7.61 (m, 1H, Ar-H), 7.37-7.40 (m, 1H, Ar-H), 7.18-7.19 (m, 1H, Ar-H), 6.89-6.90 (m, 1H, Ar-H), 3.88-3.90 (m, 4H, CH_2), 3.41 (s, 6H, CH_3), 1.72 (s, 6H, CH_2); ^{13}C-NMR (100MHz, $CDCl_3$) **δ** ppm 147.1, 145.6, 134.2, 133.1, 120.2, 116.6, 115.6, 114.7, 112.2, 110.7, 106.9, 63.6, 59.3, 56.4, 43.6, 33.3, 22.7, 21.5, 20.7, 19.7, 18.7, 12.7, 12.12; HRMS (TOF MS ES$^+$): calcd for $C_{19}H_{22}N_3O^+$: m/z 308.1757 ([M]$^+$), found: m/z 308.1742 [M]$^+$.

9-(ethylamino)-10-methyl-5*H*-benzo[a]phenoxazin-5-iminium chloride (Ox12): The compound was prepared as reported previously.(Frade et al., 2008, Frade et al., 2006) Yield (0.7 g, 83 %); mp: 260 °C; ^{1}H-NMR (D_2O, 70 °C) **δ** ppm 8,4 (s, 1H), 8.1 (br s, 1H), 7.9 (s, 1H), 7.3 (s, 1H), 7.2 (s, 1H), 6.7 (s, 2H), 6.5 (s, 1H), 3.73 (s, 3H), 2.36 (m, 2H), 1.64 (m, 3H); ^{13}C-NMR (DMSO-d_6): **δ** ppm 161.49, 160.44, 153.63, 150.70, 146.59, 133.84, 133.72, 130.64, 127.72, 126.72, 125.04, 118.53,

114.85, 108.31, 95.26, 93.29, 37.75, 16.95, 13.48; LCMS ESI TOF: calcd for $C_{19}H_{18}N_3O^+$: m/z 304.14 ($[M+H]^+$), found: m/z 304.4 $[M+H]^+$.

9-(diethylamino)-5*H*-pyrido[3,2-a]phenoxazin-5-iminium chloride (Ox17): To a round bottom flask, 5-(diethylamino)-2-nitrosophenol (2.7 mmol) and quinolin-8-amine (2.7 mmol) were dissolved in ethanol (20 mL). To the solution, concentrated HCl (0.1 mL, 37%) was added. The mixture was heated to reflux for 72 h with stirring. After heating, the reaction was cooled to room temperature with a residue obtained by filtration. The residue was then dissolved in distilled water (40 mL) and the solution was adjusted to pH~9.0 by the slow addition of ammonia. The basic mixture was stirred for 3 h at room temperature, and then filtered. Purification was achieved using silica column chromatography using CH_2Cl_2 /MeOH as the solvent system to provide the pure dye. Yield 56%; mp: 247-249 °C; ^{1}H-NMR (MeOD-*d*$_4$): **δ** ppm 9.12 (m, 1H), 9.02 (m, 1H), 7.85-9.05(m, 2H), 7.33 (m, 1H), 6.99 (m, 1H), 3.73 (m, 4H), 1.37 (m, 6H); ^{13}C-NMR (MeOD-*d*$_4$): **δ** ppm 162.38, 161.39, 153.67, 151.54, 147.73, 134.49, 134.15, 132.33, 128.49, 125.86, 118.67, 114.78, 113.90, 108.77, 95.45, 45.40, 11.55; HRMS (TOF MS ES$^+$): calcd for $C_{19}H_{19}N_4O^+$: m/z 319.1553 ($[M]^+$), found: m/z 319.1230 $[M]^+$.

9-(ethylamino)-6,10-dimethyl-5*H*-benzo[a]phenoxazin-5-iminium chloride (Ox14): The 2-methylnaphthalen-1-amine was dissolved in ethanol and cooled to 0 °C. To this was added 5-(ethylamino)-4-methyl-2-nitrosophenol and conc. HCl (0.05 mL). The mixture was refluxed for 3.5 h and monitored by TLC using CH_2Cl_2 and MeOH as solvent. After complete conversion of the starting materials, the reaction was quenched by adding 5% $NaHCO_3$ and extracted with ethyl acetate. Purification was achieved using silica gel column chromatography using CH_2Cl_2/MeOH (9/1) as the solvent system to provide the pure dye. Yield (0.83 g, 73 %); mp: 225-230 °C; ^{1}H-NMR (D_2O, 70 °C) **δ** ppm 7.86 (s, 1H), 7.67 (s, 3H), 6.63 (s, 1H), 5.93 (s, 1H), 3.28 (s, 2H), 2.06 (s, 3H), 1.87 (s, 3H), 1.52 (s, 3H); ^{13}C-NMR (MeOD) **δ** ppm 176.00, 157.09, 131.53, 131.10, 129.00, 123.44, 122.24, 121.14, 95.83, 48.45, 37.51, 16.08, 12.74; HRMS (TOF MS ES$^+$): calcd for $C_{20}H_{20}N_3O^+$: m/z 318.16 ($[M]^+$), found: m/z 318.1 $[M]^+$.

9-(ethylamino)-2-hydroxy-10-methyl-5*H*-benzo[a]phenoxazin-5-iminium chloride (Ox13): The compound was prepared as reported previously.(Firmino et al., 2014) Yield (0.83 g, 73%); mp:

255 – 260 °C; ^{1}H-NMR (DMSO-d_6, 70 °C) **δ** ppm 10.94 (br s, 1H), 9.70 (br s, 1H), 8.39 – 8.37 (d, J = 8.0 Hz, 1H), 8.09 (s, 1H), 7.57 (s, 1H), 7.32 – 7.25 (m, 2H), 6.81 – 6.78 (m, 1H), 3.43 (s, 2H), 2.27 (s, 3H), 1.27 (s, 3H); ^{13}C-NMR (DMSO-d_6): 162.30, 161.26, 154.44, 151.50, 147.39, 134.66, 131.44, 127.51, 125.85, 119.34, 115.63, 109.13, 96.09, 94.09, 49.03, 38.55, 17.71, 14.26; LCMS ESI TOF: calcd for $C_{50}H_{65}N_4O_8S_3^+$: m/z 946.4031([M+H]$^+$), found: m/z 473.1717 [M+H]$^{2+}$. Lit. mp: >300 °C.

9-(diethylamino)-2-hydroxy-5*H*-benzo[a]phenoxazin-5-iminium chloride (Ox16): The compound was prepared as reported previously.(Liu et al., 2014) Yield (43%). mp: >260 °C ^{1}H-NMR (DMSO-d_6): **δ** ppm 11.05 (s, 1H), 9.12 (brs, 1H), 9.79 (s, 1H), 8.37 (d, J = 9Hz, 1H), 8.12 (s, 1H), 7.79 (d, J = 9 Hz, 1H), 7.27 (m, 1H), 7.16 (m, 1H), 6.96 (s, 1H), 6.76 (s, 1H), 3.64 (m, 4H), 1.22 (m, 6H), ^{13}C-NMR (MeOD-d_4): **δ** ppm 162.38, 161.39, 153.67, 151.54, 147.73, 134.49, 134.15, 132.33, 128.49, 125.86, 118.67, 114.78, 113.90, 108.77, 95.45, 45.40, 11.55; HRMS (TOF MS ES$^+$): calcd for $C_{20}H_{20}N_3O_2^+$: m/z 334.1550 ([M]$^+$), found: m/z 334.1465 [M]$^+$; Lit. Yield: 50.5%, mp: >300 °C.

dimethyl-3,3'-((5-oxo-5*H*-benzo[a]phenoxazine-9-yl)azanediyl)dipropionate (Ox34): The compound was prepared as reported previously.(Jose and Burgess, 2006) mp: > 260 °C; ^{1}H-NMR (DMSO-d_6): δ ppm 10.54 (s, 1H), 7.96 (d, J = 8.8 Hz, 1H), 7.88 (s, 1H), 7.59 (d, J = 9.2 Hz, 1H), 7.09 (dd, 1H), 6.81 (dd, 1H), 6.70 (d, J = 2.4 Hz, 1H), 6.15 (s, 1H), 3.73 (t, J = 7.2 Hz, 4H), 3.62 (s, 1H), 2.652 (t, J = 7.2 Hz, 4H); ^{13}C-NMR (DMSO-d_6): δ ppm 181.68, 171.74, 160.69, 151.48, 150.19, 146.11, 139.98, 133.61, 130.70, 127.50, 124.27, 123.85, 118.59, 110.06, 108.30, 104.42, 96.98, 51.53, 46.30, 31.46; LCMS ESI TOF: calcd for $C_{24}H_{22}N_2O_7^+$: m/z 473.1319 ([M+Na]$^+$), found: m/z 473.1456 [M+Na]$^+$; Lit. Yield: 60%.

9-(bis(3-methoxy-3-oxopropyl)amino)-2-hydroxy-5*H*-benzo[a]phenoxazin-5-iminium chloride (Ox37): To a round bottom flask, 6-aminonaphthol (2.7 g, 16.9 mmol) was added to a solution of dimethyl-3,3'-((3-hydroxy-4-nitrosophenyl)azanediyl)dipropionate (5.24 g, 16.9 mmol) in DMF (20 mL). The reaction mixture was refluxed for 3 h. The solvent was evaporated, and the residue was purified by column chromatography using CH_2Cl_2 /MeOH as the solvent system to afford the compound. mp: > 260 °C; ^{1}H-NMR (DMSO-d_6) **δ** ppm 11.14 (s, 1H), 10.13 (br s, 2H),

8.41 (d, J = 8.8 Hz, 1H), 8.11 (s, 1H), 7.81 (t, J = 5.6 Hz, 1H), 7.29 (d, J = 8.8 Hz, 1H), 7.16 (br s, 1H), 7.02 (s, 1H), 6.79 (s, 1H), 3.84 (t, J = 6.4 Hz, 4H), 3.63 (s, 6H), 2.72 (t, J = 7.2 Hz, 4H); HRMS (TOF MS ES$^+$): calcd for $C_{24}H_{24}N_3O_6^+$: m/z 450.1660 ([M]$^+$), found: m/z 450.1071 [M]$^+$.

9-(ethylamino)-2-methoxy-10-methyl-5*H*-benzo[a]phenoxazin-5-iminium chloride (Ox116): To a clean dried 50 mL round bottom flask, 6-Methoxynaphthalen-1-amine (0.38 g, 2.1 mmol) was dissolved in ethanol and cooled to 0 °C. To this was added 5-(ethylamino)-4-methyl-2-nitrosophenol (0.45 g, 2.0 mmol) and conc. HCl (0.05 mL). The mixture was refluxed for 5 h and monitored by TLC using CH_2Cl_2/MeOH as solvent. After complete conversion of the starting materials, the reaction was quenched by adding 5% $NaHCO_3$ and extracted with ethyl acetate. Purification was achieved using silica gel column chromatography with the solvent system CH_2Cl_2/MeOH (9/1) to provide the pure compound. Yield (0.52 g, 70 %); mp: > 260 °C; ^{1}H-NMR (MeOD) δ ppm 8.27 – 8.21 (d, J = 8.0 Hz, 1H), 7.62 – 7.60 (d, J = 2.0 Hz, 1H), 7.39 – 7.33 (m, 2H), 6.75 (s, 1H), 5.85 (s, 1H), 4.04 (s, 1H), 2.32 (s, 3H), 1.36 (s, 7H); ^{13}C-NMR (DMSO-d_6) δ ppm 161.97, 157.60, 154.70, 151.46, 147.59, 133.35, 133.16, 131.47, 129.29, 126.64, 126.26, 118.55, 117.54, 105.62, 93.70, 92.53, 56.19, 38.61, 17.84, 14.23; HRMS (TOF MS ES$^+$): calcd for $C_{20}H_{20}N_3O_2^+$: m/z 334.15 ([M]$^+$), found: m/z 334.1 [M]$^+$.

(*E*)-*N*-(9-(ethylamino)-2-methoxy-10-methyl-5*H*-benzo[a]phenoxazin-5-ylidene)methan aminium chloride (Ox117): To a clean dried 50 mL round bottom flask, *6-methoxy-N-methylnaphthalen-1-amine* (0.25 g, 1.33 mmol) was dissolved in ethanol and cooled to 0 °C. To this solution was added 5-(ethylamino)-4-methyl-2-nitrosophenol (0.29 g, 1.33 mmol) and conc. HCl (0.05 mL). The mixture was refluxed for 5 h and monitored by TLC using CH_2Cl_2 and MeOH as solvent. After complete conversion of the starting materials, the reaction was quenched by adding 5 % $NaHCO_3$ and extracted with ethyl acetate. Purification was achieved using silica gel column chromatography with the solvent system CH_2Cl_2/MeOH (9/1) to provide the pure compound. Yield (0.32 g, 70%); mp: 220-225 °C; ^{1}H-NMR (DMSO) **δ** ppm 10.19 (br s, 1H), 8.45 – 8.43 (d, J = 8.0 Hz, 1H), 7.82 (s, 1H), 7.62 (s, 1H), 7.44 (s, 1H), 7.28 – 7.26 (d, 1H), 6.60 – 6.54 (m, 2H), 3.92 (s, 2H), 3.17 (s, 3H), 2.22 (s, 3H), 1.28 – 1.25 (t, 3H); ^{13}C-NMR (DMSO) **δ** ppm 161.97, 157.40, 154.70, 151.46, 147.59, 133.35, 133.16, 131.47, 129.29, 126.64, 126.26, 118.55, 117.54, 105.62,

93.70, 92.53, 56.19, 38.61, 31.64, 17.84, 14.23; HRMS (TOF MS ES$^+$): calcd for $C_{21}H_{22}N_3O_2^+$: m/z 348.17 ([M]$^+$), found: m/z 334.1 [M]$^+$.

3-((9-(diethylamino)-5-iminio-5*H*-benzo[a]phenoxazin-3-yl)oxy)propane-1-sulfonate (Ox27): To a round bottom flask, 5-(diethylamino)-2-nitrosophenol (2.7 mmol) and the appropriate 5-aminonaphthalene (2.7 mmol) were dissolved in ethanol (20 mL). To the solution, concentrated HCl (0.1 mL, 37%) was added. The mixture was heated to reflux for 72 h with stirring. After heating, the reaction was cooled to room temperature with a residue obtained by filtration. The residue was then dissolved in distilled water (40 mL) and the solution was adjusted to pH~9 by the slow addition of ammonia. The basic mixture was stirred for 3 h at room temperature, and then filtered. Purification was achieved using silica column chromatography using CH_2Cl_2/MeOH as the solvent system to provide the pure dye. Yield (13%); mp: >260 °C; ^{1}H-NMR (DMSO-d_6): **δ** ppm 10.66 (br s, 1H), 10.35 (br s, 1H), 8.68 (d, J = 9 Hz, 1H), 7.83 (m, 2H), 7.44 (m, 1H), 7.22 (m, 1H), 7.10 (s, 1H), 6.94 (s, 1H), 3.86 (m, 2H), 3.63 (m, 4H), 2.65 (m, 2H), 2.07 (m, 2H), 1.22 (m, 6H); ^{13}C-NMR (DMSO-d_6): **δ** ppm 161.64, 159.97, 153.01, 151.10, 147.79, 135.24, 132.33, 128.98, 126.74, 125.14, 123.98, 122.33, 114.83, 109.54, 97.32, 96.23, 45.55, 13.00; HRMS (TOF MS ES$^+$): calcd for $C_{23}H_{25}N_3NaO_5S^+$: m/z 478.1407 ([M+Na]$^+$), found: m/z 478.1204 [M+Na]$^+$.

Protein conjugation with ZW800-1: Cyclic pentapeptide cyclo (Arg-Gly-Asp-DTyr-Lys; cRGD; MW 619.6) was synthesized as previously reported, and conjugated to ZW800-1 using *N*-hydroxysuccinimide (NHS) ester chemistry in DMSO.(Choi et al., 2010) NIR fluorophores were also conjugated to GLP-1 (Abcam, Cambridge, MA) in PBS, pH 7.8, followed by purification by gel filtration chromatography. *In silico* calculations of the partition coefficient (log*D*) and surface molecular charge and hydrophobicity were calculated using MarvinSketch 5.2.1 (ChemAxon, Budapest, Hungary).

Optical and physicochemical property analyses

All optical measurements were performed at 37 °C in PBS, pH 7.4 or 100% FBS buffered with 50 mM HEPES, pH 7.4. Absorbance and fluorescence emission spectra of the series of NIR fluorophores were measured using fiber optic HR2000 absorbance (200–1100 nm) and USB2000FL fluorescence (350–1000 nm) spectrometers (Ocean Optics, Dunedin, fL). NIR excitation was provided by a 655 nm red laser pointer (Opcom Inc., Xiamen, China) set to 5 mW and coupled through a 300 μm core diameter, NA 0.22 fiber (Fiberguide Industries, Stirling, NJ). For fluorescence quantum yield (QY) measurements, oxazine 725 in ethylene glycol (QY = 19%) was used as a calibration standard, under conditions of matched absorbance at 655 nm. *In silico* calculations of the partition coefficient (Log*D* at pH 7.4), surface molecular charge, hydrophobicity, hydrogen bond acceptors/donors (HBA/HBD), and total polar surface area (TPSA) were calculated using Marvin and JChem calculator plugins (ChemAxon, Budapest, Hungary).

Cell membrane binding assay

NIT-1 (ATCC, Manassas, VA) were seeded onto 16-well plates and incubated at 37°C in humidified 5% CO_2 incubator in F12K and DMEM, respectively, supplemented with 10% FBS and 1% Pen/Strep. When cells reached ≈ 80% confluence, they were rinsed twice with PBS then MB or Ox61 was added to each well at a concentration of 2 μM and incubated for 1 h at 37°C in a humidified 5% CO_2 incubator. Cells were washed 3 times with culture media prior to imaging. After imaging, periodic acid at a concentration of 0.1 mM was added and images were taken immediately after. The cells were observed on a 4-channel NIR fluorescence microscope. The excitation and emission filter used for microscopy was 650 ± 22 nm and 710 ± 25 nm, respectively.

Plasma protein binding test

The RED device was purchased from Thermo Fisher (Waltham, MA) and the plasma protein binding assay was performed following the detailed instruction provided by the manufacture.(Brouwer et al., 2000) 200 μL of samples were prepared in mouse plasma serum at 10 μM. The samples were added into the sample chamber and 400 μL of PBS buffer (pH 7.4) was added to the buffer chamber. The plate was sealed with sealing tape and incubated at 37°C on a shaker at 150 rpm for 4 h. Equal volume from both the buffer and the plasma chambers were collected for samples analysis.

Fluorescence signals of each chamber were measured to calculate the percentage of bound and unbound fractions for each sample.

NIR fluorescence imaging system

For the NIR fluorescence imaging, the FLARE system has been described in detail previously.(Choi et al., 2013, Gioux et al., 2010) In this study, a 670 nm excitation was used at a fluence rate of 2 mW/cm^2, with white light (400 – 650 nm) at 12,000 lx. Color and NIR fluorescence images were acquired simultaneously with custom software at rates up to 15 Hz over a 10 cm diameter field-of-view (FOV). A pseudo-colored lime green was used for NIR fluorescence in the color-NIR merged images. The imaging system was positioned at a distance of 9 inches from the surgical field. For all real-time intraoperative imaging, a standardized imaging protocol was used during and after the operation. General FOV (5 cm in dia.) was used to include pancreas head, duodenum, liver, and kidneys of a mouse, while closeup FOV (3.3 cm in dia.) includes pancreas head and duodenum. Color and NIR fluorescence images were taken simultaneously.

Animal models and intraoperative fluorescence imaging

Animals were housed in an AAALAC-certified facility. Animal studies were performed under the supervision of BIDMC IACUC in accordance with approved institutional protocols (#101-2011). 4 wk old insulinoma-bearing NOD/ShiLt-Tg(RipTAg)1Lt/J mice (both male and female) were purchased from Jackson Laboratories (Bar Harbor, ME). Insulinoma-bearing mice were maintained on a high glucose diet (8.4 g sugar in 250 mL water) until they were ready for intraoperative tumor targeting study. Animals were anesthetized with 100 mg/kg ketamine and 10 mg/kg xylazine intraperitoneally (Webster Veterinary, Fort Devens, MA). Following anesthesia, a midline incision was made to expose the abdominal cavity and head of the pancreas. For kinetics and dose-response studies, 0.3 to 6.0 mg/kg of MB or Ox61 in saline were injected intravenously into insulinoma-bearing tumor mice, and images were taken over 4 h ($n = 5$, mean ± s.d.). Control images were acquired prior to injecting NIR fluorophores. The fluorescence signal in tumors (Tu) and tumor-to-background ratio (TBR) compared to neighboring pancreas (Pa) was obtained over the period of imaging. For tumor stage targeting, insulinoma-bearing mice from 5 to 13 wk old were administered with 0.3-6.0 mg/kg of Ox61 in saline. Real-time signal accumulation at tumor site was observed over 30 min post-injection of 1.5 mg/kg of Ox61, and the fluorescence intensity was plotted to

evaluate *in vivo* molecular biodistribution and clearance. Animals were sacrificed 1-4 h post-injection, and pancreas and tumorous tissues were resected for *ex vivo* imaging and histology.

In vivo biodistribution and clearance

Before the surgery, mice were anesthetized with ketamine (100 mg/kg) and xylazine (10 mg/kg) through intraperitoneal injection. Midline incision was performed to open abdominal cavity. For all real-time tumor imaging, a standardized imaging protocol was used during and after the operation. General FOV included pancreas head, duodenum, liver, and kidney. 1.5 mg/kg of MB and Ox61 were injected intravenously into 25 g male CD-1 mice, and images were taken for 4 h.

Magnetic Resonance Imaging (MRI)

1T micro MRI scanner (Aspect, Israel) was used to track tumor growth noninvasively and longitudinally.(Kim et al., 2013) Insulinoma-bearing mice were scanned once every week starting at 5 wk to 14 wk old of age. In order to optimize the MR protocol, T1-weighed spin echo, T2-weighed spin echo, and gradient echo sequences were compared using the same insulinoma-bearing mouse. T2-weighed fast-spin echo (FSE) sequence was used to localize tumor with echo time (TE) of 80 ms and repetition time (TR) of 4,000 ms using 4 NEX, 256 x 256 matrix, and 1 mm slice thickness. MRI images were analyzed using VivoQuant 1.22 software.

Histology and immunohistochemistry (IHC)

Pancreas was embedded in Tissue-Tek OCT compound (Fisher Scientific) without a pre-fixation step and the tissue solidified at – 80°C. Frozen samples were cryosectioned (10 μm per slice) and fixed in acetone; 1 slide was stained with H&E and consecutive sections were used for fluorescence microscopy and IHC. For IHC, Exendin-4 (GLP-1 agonist; Abcam) conjugated with ZW800-1 was used to visualize pancreatic islet cell tumors. Fluorescence imaging was conducted using a Nikon TE2000 epifluorescence microscope equipped with a 75 W xenon light source, NIR-compatible optics, and a NIR-compatible 4X, 10X, 20X, and 40X Plan Fluor objective lens (Nikon, Melville, NY). Images were acquired on an Orca-AG (Hamamatsu, Bridgewater, NJ). Image acquisition and analysis was performed using IPLab software (Scanalytics, Fairfax, VA). A custom filter set (Chroma Technology Corporation, Brattleboro, VT) composed of a 650/45 nm excitation filter, a 685 nm dichroic mirror, and a 720/60 nm emission filter were used for imaging.

Quantitative analysis

At each time point, the fluorescence and background intensity of a region of interest (ROI) over each tissue was quantified using custom FLARE software. The signal-to-background ratio (SBR) was calculated as SBR = target signal/background signal, where background is surrounding tissue. The TBR was calculated as tumor fluorescence/background signal, where background is the signal intensity of neighboring pancreas obtained over the imaging period. All NIR fluorescence images were normalized identically for all conditions of an experiment. At least 5 animals were analyzed at each experimental condition. Statistical analysis was carried out using a one-way ANOVA followed by Tukey's multiple comparisons test. *P* values less than 0.05 were considered significant: $*P < 0.05$, $**P < 0.01$, and $***P < 0.001$. The experiments were not randomized, and the investigators were not blinded to allocation during experiments and outcome assessment. Results were presented as mean ± s.d. and curve fitting was performed using Microsoft Excel and Prism version 4.0a software (GraphPad, San Diego, CA).

Intravital laser-scanning microscopy

Under ketamine-xylazine anesthesia, the insulinoma-bearing mice were mounted on a heated stage. The pancreas was placed under the upright water immersion objective lens (20X, 1.0 NA) of a custom-built, video-rate (30 Hz), laser-scanning two-photon microscope. Both FITC-dextran (2 MDa MW) and Ox61 were excited by 150 fs pulses centered at 800 nm from a Ti:Sapphire laser. The average power was tuned to ~ 20 mW at the sample. The microscope has 3 simultaneous detection channels comprising dielectric optical filters and photomultiplier tubes. The two-photon excited fluorescence from Ox61 was collected with a band-pass filter at 600 ± 50 nm, and the fluorescence from FITC-dextran was detected with a 525 ± 25 nm filter. Images were acquired by averaging 30 video frames (1 s). The images were analyzed using ImageJ version 1.45q software.

REFERENCES

Brouwer, E., Verweij, J., De Bruijn, P., Loos, W. J., Pillay, M., Buijs, D. & Sparreboom, A. 2000. Measurement of fraction unbound paclitaxel in human plasma. *Drug Metab Dispos,* 28**,** 1141-5.

Choi, H. S., Gibbs, S. L., Lee, J. H., Kim, S. H., Ashitate, Y., Liu, F., Hyun, H., Park, G., Xie, Y., Bae, S., Henary, M. & Frangioni, J. V. 2013. Targeted zwitterionic near-infrared fluorophores for improved optical imaging. *Nat. Biotechnol.,* 31**,** 148-53.

Choi, H. S., Liu, W., Liu, F., Nasr, K., Misra, P., Bawendi, M. G. & Frangioni, J. V. 2010. Design considerations for tumour-targeted nanoparticles. *Nat Nanotechnol,* 5**,** 42-7.

Firmino, P. R., Mattos Neto, P. S. & Ferreira, T. A. 2014. Correcting and combining time series forecasters. *Neural Netw,* 50**,** 1-11.

Frade, V. H., Sousa, M. J., Moura, J. C. & Goncalves, M. S. 2008. Synthesis of naphtho[2,3-a]phenoxazinium chlorides: structure-activity relationships of these heterocycles and benzo[a]phenoxazinium chlorides as new antimicrobials. *Bioorg Med Chem,* 16**,** 3274-82.

Frade, V. H. J., Goncalves, M. S. T., Coutinho, P. J. G. & João, C. V. P. 2006. Synthesis and spectral properties of long-wavelength fluorescent dyes. *Journal of Photochemistry and Photobiology A: Chemistry,* 185**,** 220-230.

Ge, J. F., Arai, C., Kaiser, M., Wittlin, S., Brun, R. & Ihara, M. 2008. Synthesis and in vitro antiprotozoal activities of water-soluble, inexpensive 3,7-bis(dialkylamino)phenoxazin-5-ium derivatives. *J Med Chem,* 51**,** 3654-8.

Gioux, S., Choi, H. S. & Frangioni, J. V. 2010. Image-guided surgery using invisible near-infrared light: fundamentals of clinical translation. *Mol. Imaging,* 9**,** 237-55.

Jose, J. & Burgess, K. 2006. Syntheses and Properties of Water-Soluble Nile Red Derivatives. *The Journal of Organic Chemistry,* 71**,** 7835-7839.

Kim, S. H., Lee, J. H., Hyun, H., Ashitate, Y., Park, G., Robichaud, K., Lunsford, E., Lee, S. J., Khang, G. & Choi, H. S. 2013. Near-infrared fluorescence imaging for noninvasive trafficking of scaffold degradation. *Sci Rep,* 3**,** 1198.

Liu, X. D., Fan, C., Sun, R., Xu, Y. J. & Ge, J. F. 2014. Nile-red and Nile-blue-based near-infrared fluorescent probes for in-cellulo imaging of hydrogen sulfide. *Anal Bioanal Chem,* 406**,** 7059-70.

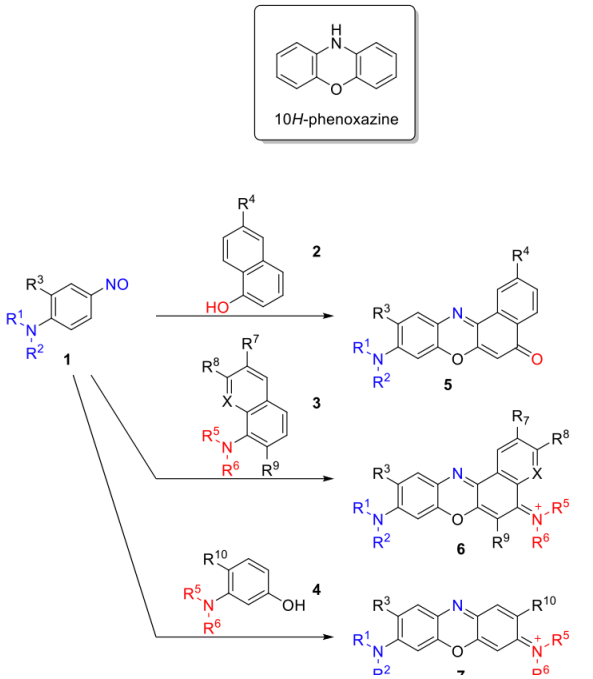

5: **Ox34**: $R^1 = R^2 = (CH_2)_2COOCH_3$; $R^3 = H$; $R^4 = OH$

6: **Ox12**: $R^1 = Et$; $R^2 = H$; $R^3 = Me$; $R^5 = R^6 = R^7 = R^8 = R^9 = H$; X = CH
Ox17: $R^1 = R^2 = Et$; $R^3 = Me$; $R^5 = R^6 = R^7 = R^8 = R^9 = H$; X = N
Ox170*: $R^1 = Et$; $R^2 = H$; $R^3 = Me$; $R^5 = Et$; $R^6 = R^7 = R^8 = R^9 = H$; X = CH
Ox14: $R^1 = Et$; $R^2 = H$; $R^3 = Me$; $R^5 = R^6 = R^7 = R^8 = H$; $R^9 = CH_3$; X = CH
Ox13: $R^1 = Et$; $R^2 = H$; $R^3 = Me$; $R^5 = R^6 = H$; $R^7 = OH$; $R^8 = R^9 = H$; X = CH
Ox16: $R^1 = R^2 = Et$; $R^3 = H$; $R^5 = R^6 = H$; $R^7 = OH$; $R^8 = R^9 = H$; X = CH
Ox37: $R^1 = R^2 = (CH_2)_2COOCH_3$; $R^3 = H$; $R^5 = R^6 = H$; $R^7 = OH$; $R^8 = R^9 = H$; X = CH
Ox116: $R^1 = Et$; $R^2 = H$; $R^3 = Me$; $R^5 = R^6 = H$; $R^7 = OMe$; $R^8 = R^9 = H$; X = CH
Ox117: $R^1 = Et$; $R^2 = H$; $R^3 = Me$; $R^5 = Me$; $R^6 = H$; $R^7 = OMe$; $R^8 = R^9 = H$; X = CH
Ox27: $R^1 = R^2 = Et$; $R^3 = R^5 = R^6 = R^7 = H$; $R^8 = O(CH_2)_3SO_3H$; $R^9 = H$; X = CH

7: **Ox61**: $R^1 = R^2 = Me$; $R^3 = H$; $R^5 = R^6 = Me$; $R^{10} = H$
Ox89: $R^1 = R^2 = Me$; $R^3 = H$; $R^5 = Et$; $R^6 = H$; $R^{10} = Me$
Ox4*: $R^1 = Et$; $R^2 = H$; $R^3 = Me$; $R^5 = Et$; $R^6 = H$; $R^{10} = Me$
Ox261: $R^1 = R^2 = Me$; $R^3 = H$; $R^5 = R^6 = Et$; $R^{10} = H$
Ox96: $R^1 = R^2 = Et$; $R^3 = H$; $R^5 = R^6 = Et$; $R^{10} = H$
Ox266: $R^1 = R^2 = Me$; $R^3 = H$; $R^5 = R^6 =$ Pyrrolidine; $R^{10} = H$
Ox269: $R^1 = R^2 = Me$; $R^3 = H$; $R^5 = R^6 =$ Piperidine; $R^{10} = H$

Figure S1. Related to Figure 1. Chemical synthesis of symmetrical and unsymmetrical phenoxazine derivatives. *Commercially available compounds.

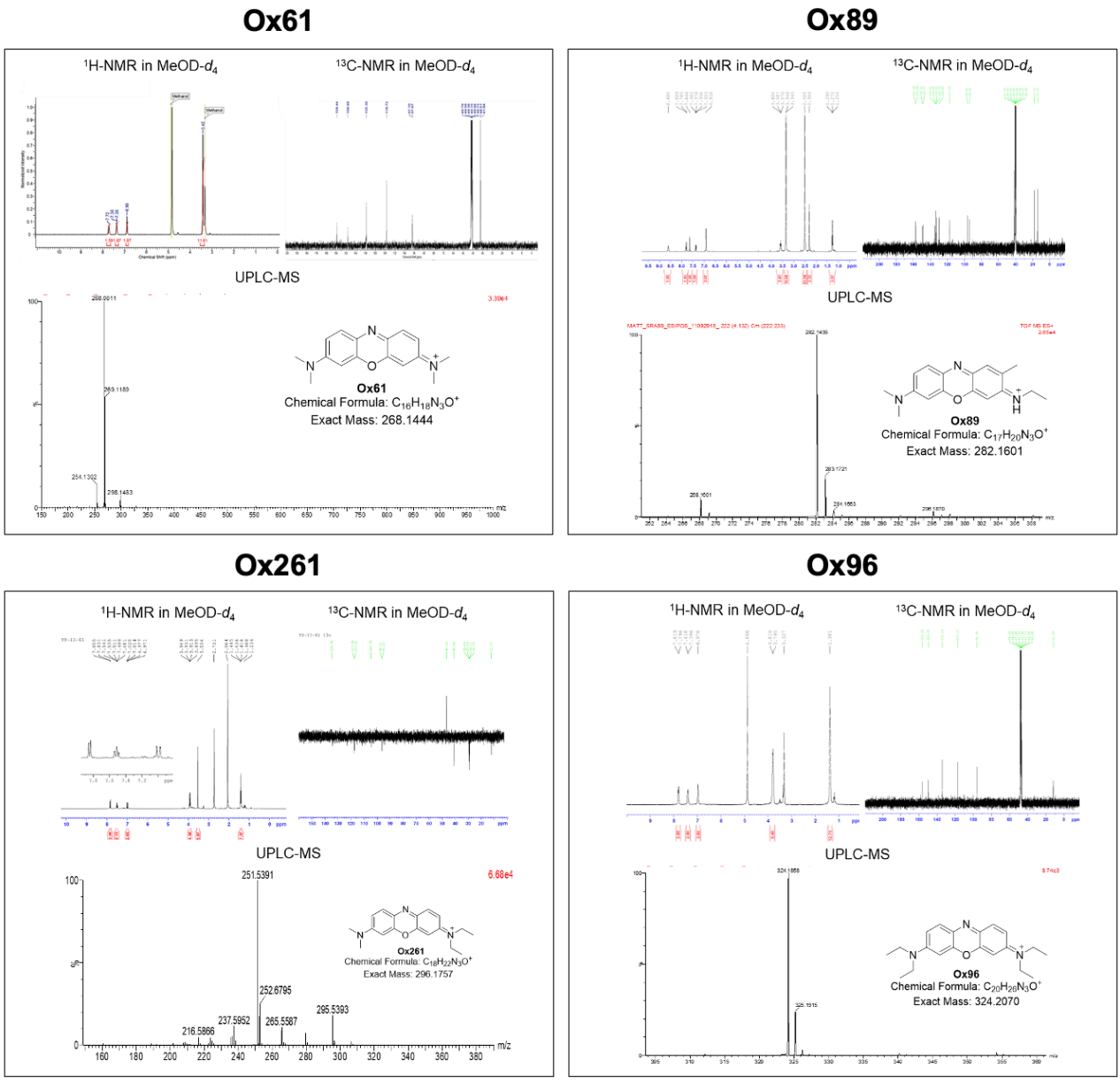

Figure S2. Chemical analysis of Ox derivatives, Related to Figure 1. ^{1}H-NMR, ^{13}C-NMR, and LC-MS analysis of phenoxazine derivatives: absorbance (photodiode array; PDA) at 210 nm, fluorescence (FLD; λ_{Exc} = 648 nm and λ_{Em} = 668 nm), and electrospray time-of-flight (ES-TOF) mass spectrometry (MS).

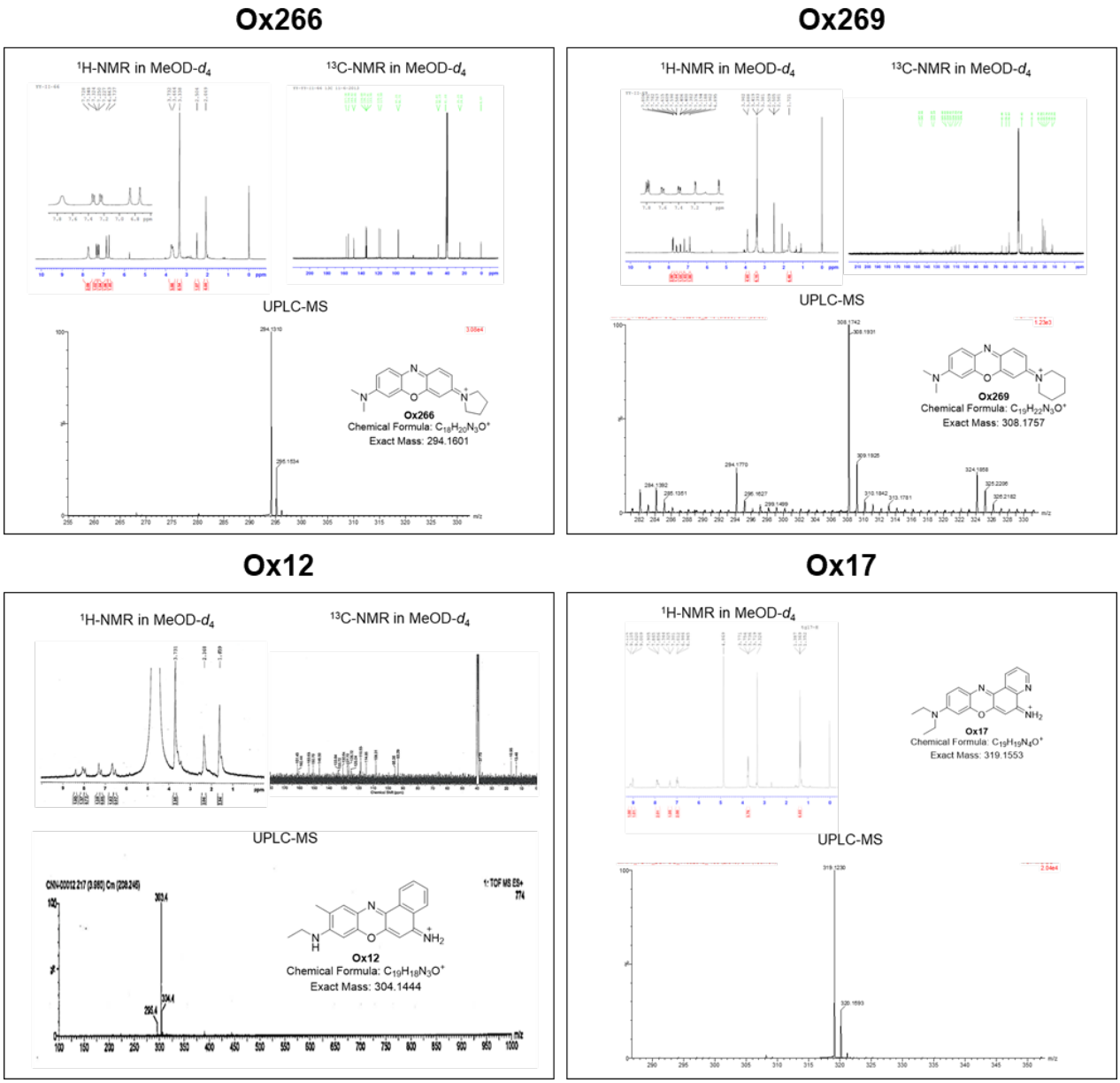

Figure S3. Chemical analysis of Ox derivatives, Related to Figure 1. ^{1}H-NMR, ^{13}C-NMR, and LC-MS analysis of phenoxazine derivatives: absorbance (photodiode array; PDA) at 210 nm, fluorescence (FLD; λ_{Exc} = 648 nm and λ_{Em} = 668 nm), and electrospray time-of-flight (ES-TOF) mass spectrometry (MS).

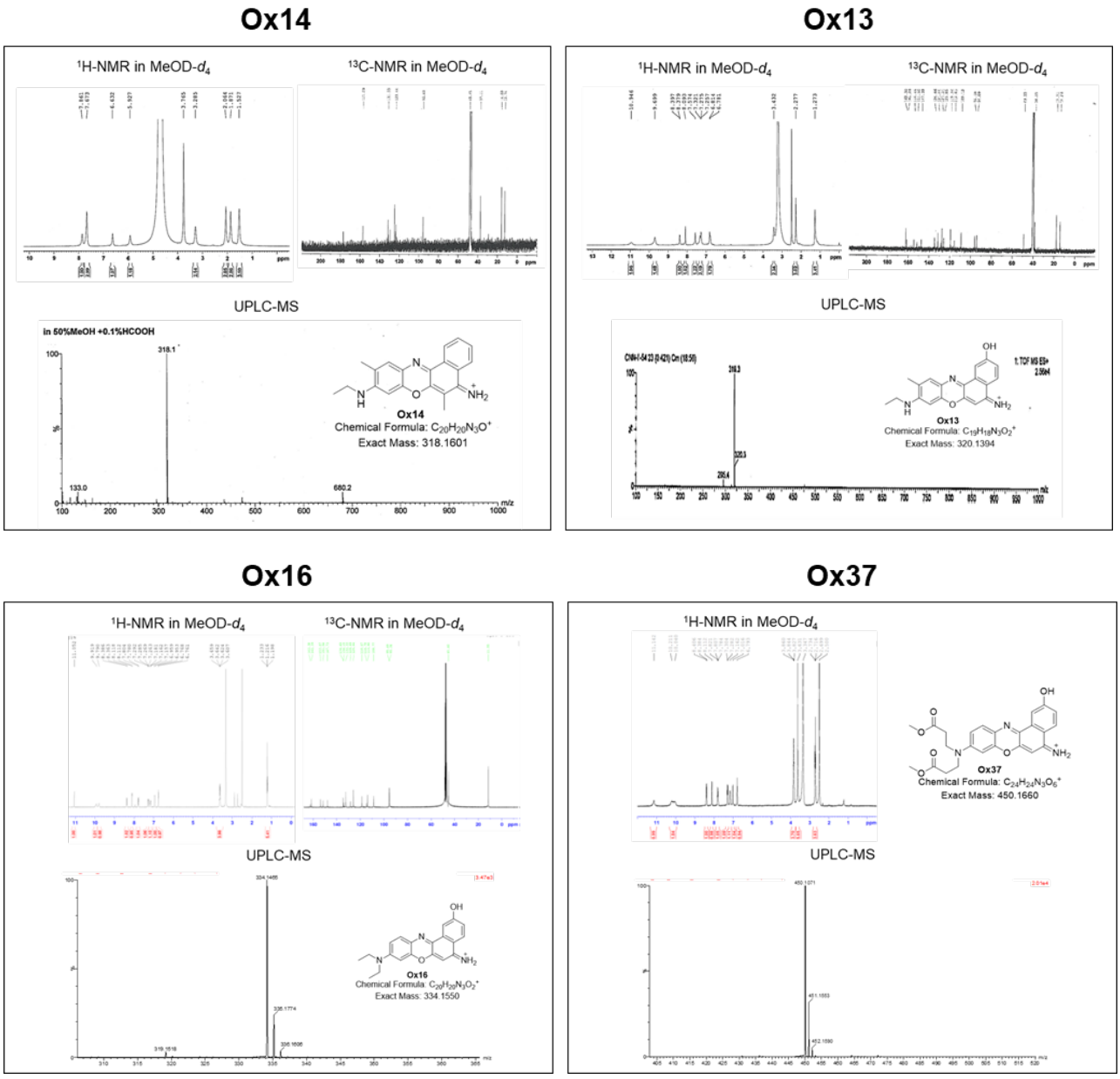

Figure S4. Chemical analysis of Ox derivatives, Related to Figure 1. ^{1}H-NMR, ^{13}C-NMR, and LC-MS analysis of phenoxazine derivatives: absorbance (photodiode array; PDA) at 210 nm, fluorescence (FLD; λ_{Exc} = 648 nm and λ_{Em} = 668 nm), and electrospray time-of-flight (ES-TOF) mass spectrometry (MS).

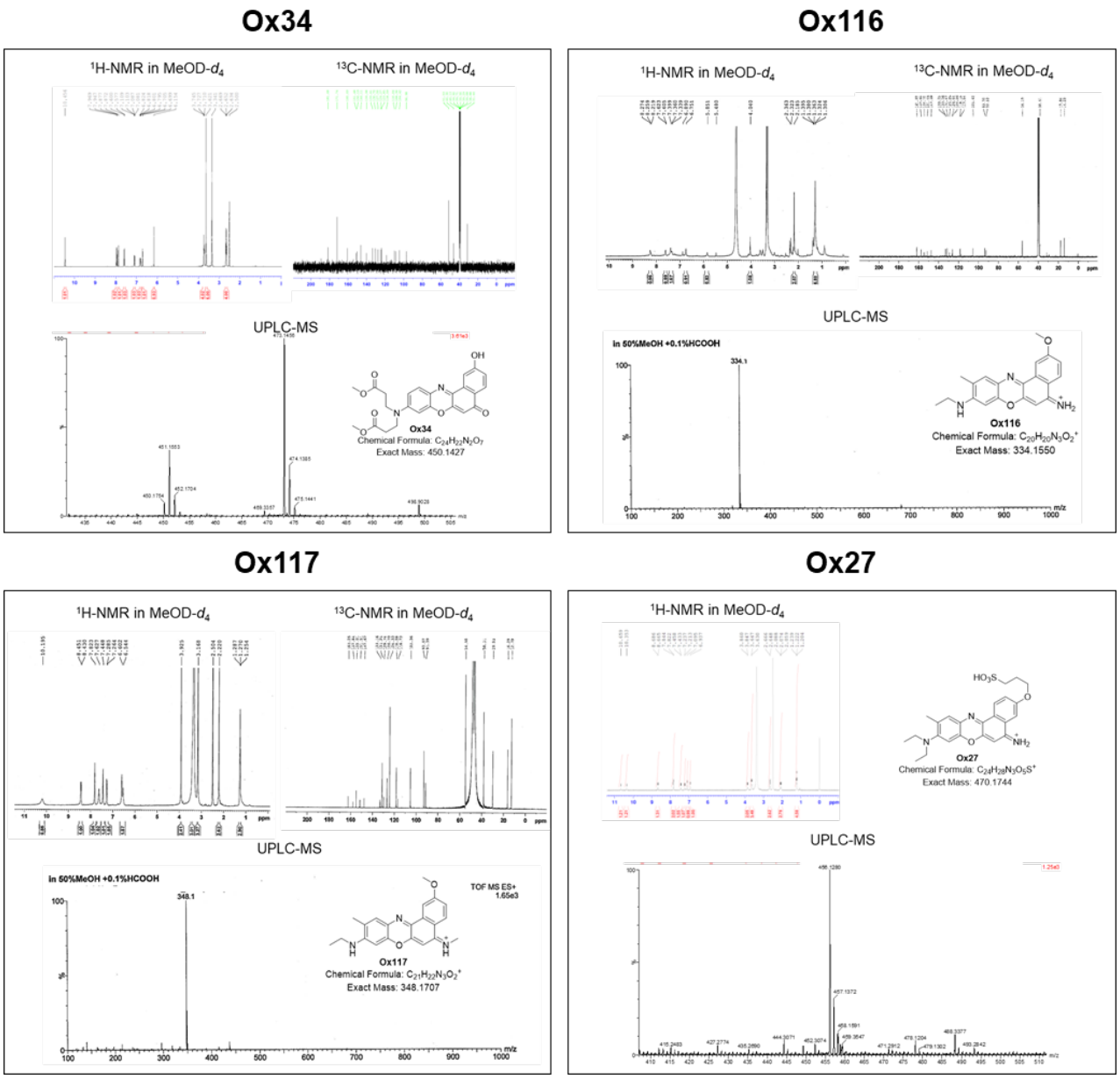

Figure S5. Chemical analysis of Ox derivatives, Related to Figure 1. ^{1}H-NMR, ^{13}C-NMR, and LC-MS analysis of phenoxazine derivatives: absorbance (photodiode array; PDA) at 210 nm, fluorescence (FLD; λ_{Exc} = 648 nm and λ_{Em} = 668 nm), and electrospray time-of-flight (ES-TOF) mass spectrometry (MS).

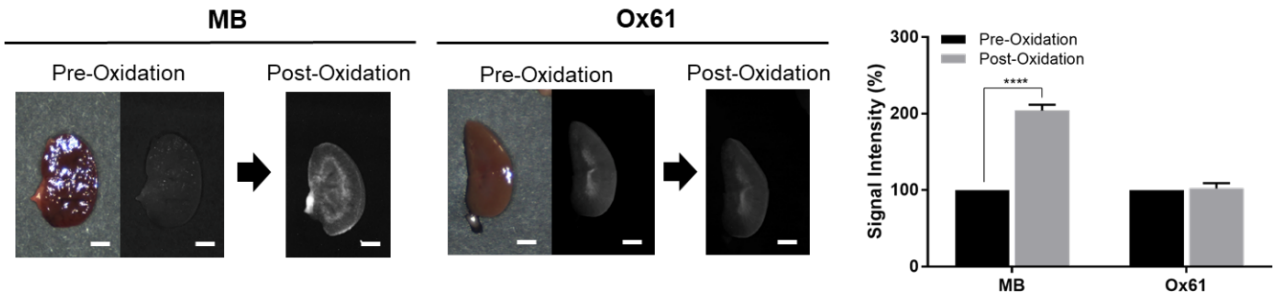

Figure S6. *Ex vivo* imaging of kidneys resected from CD-1 mice injected with 1.5 mg/kg of MB or Ox61, Related to Figure 1D. The same kidney sections were imaged again after treating with 1 mM of periodic acid and signal intensity of pre- and post-oxidation were compared (P <0.0001). Scale bars = 2 mm.

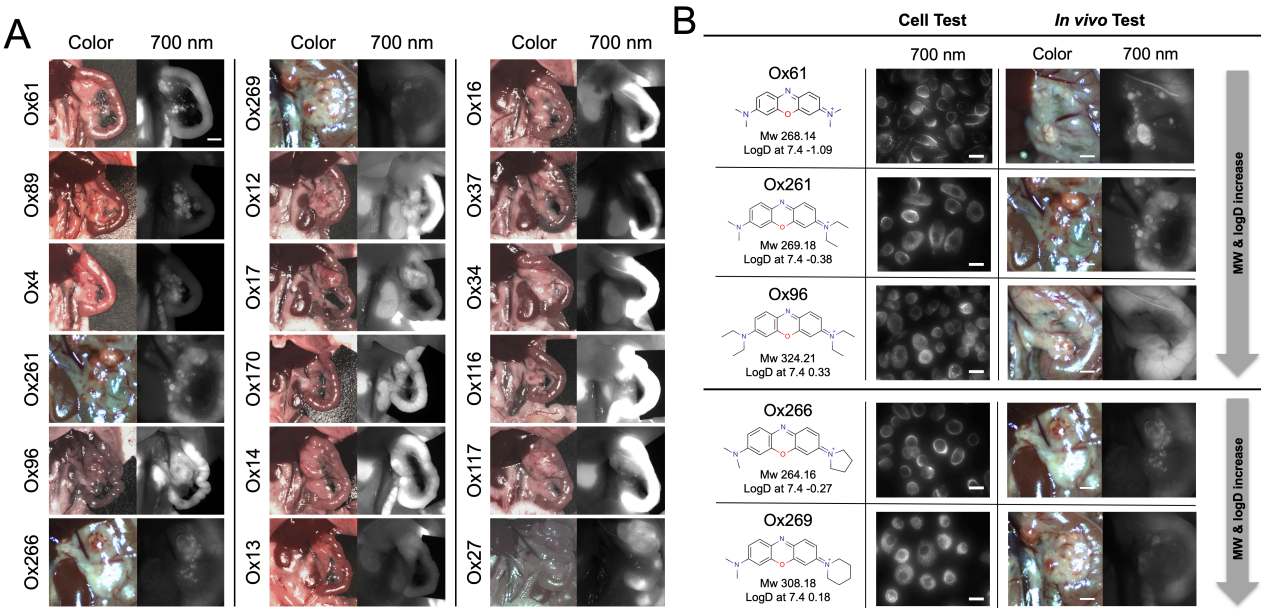

Figure S7. Tumor targetability of Ox derivatives in insulinoma mice, Related to Figure 3. **(A)** 1.5 mg/kg of Ox derivatives are injected intravenously into 13 wk old insulinoma mice and imaged 30 min post-injection. Scale bars = 3 mm. **(B)** Increase in molecular weight and log*D* by elongation of the side chain effects tumor targetability. Scale bars = 50 μm.

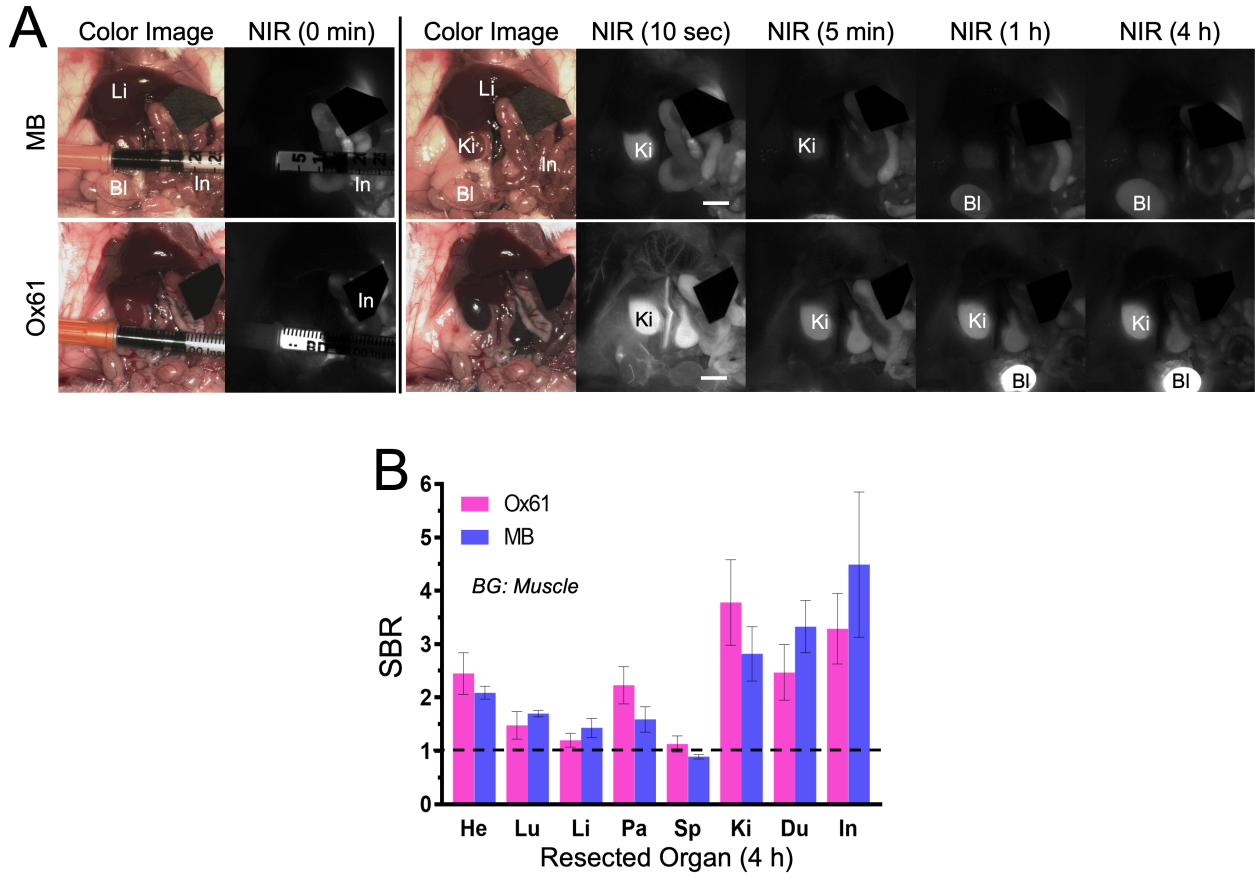

Figure S8. Kinetics optimization of MB and Ox61 in CD-1 mice, Related to Figure 3. **(A)** Intraoperative biodistribution of MB and Ox61. Scale bars = 5 mm. (**B)** Resected organs were imaged 4 h post-injection and SBR was quantified against muscle. SBR, signal-to-background ratio; He, heart; Lu, lung; Li, liver; Pa, pancreas; Sp, spleen; Ki, kidney, Du; duodenum; and In, intestine.

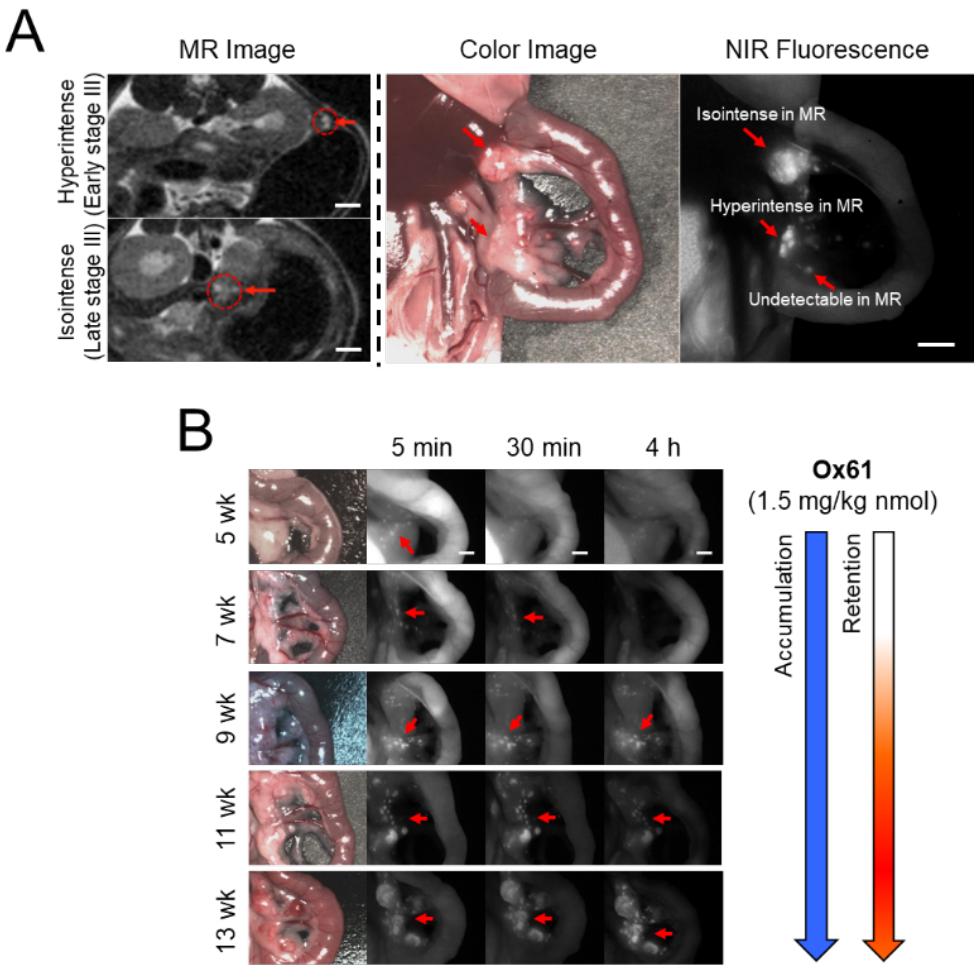

Figure S9. Intraoperative imaging of insulinomas in different stage of insulinomas, Related to Figure 3. **(A)** MR tracking and co-registration of isointense and hyperintense tumors using NIR fluorescence imaging after a single bolus injection of Ox61 (1.5 mg/kg) into insulinoma-bearing tumor mice. (**B)** Insulinoma mice from ages 5 to 13 wk were injected with 1.5 mg/kg of Ox61 and imaged 5, 30 min and 4 h post-intravenous injection. Scale bars = 3 mm.

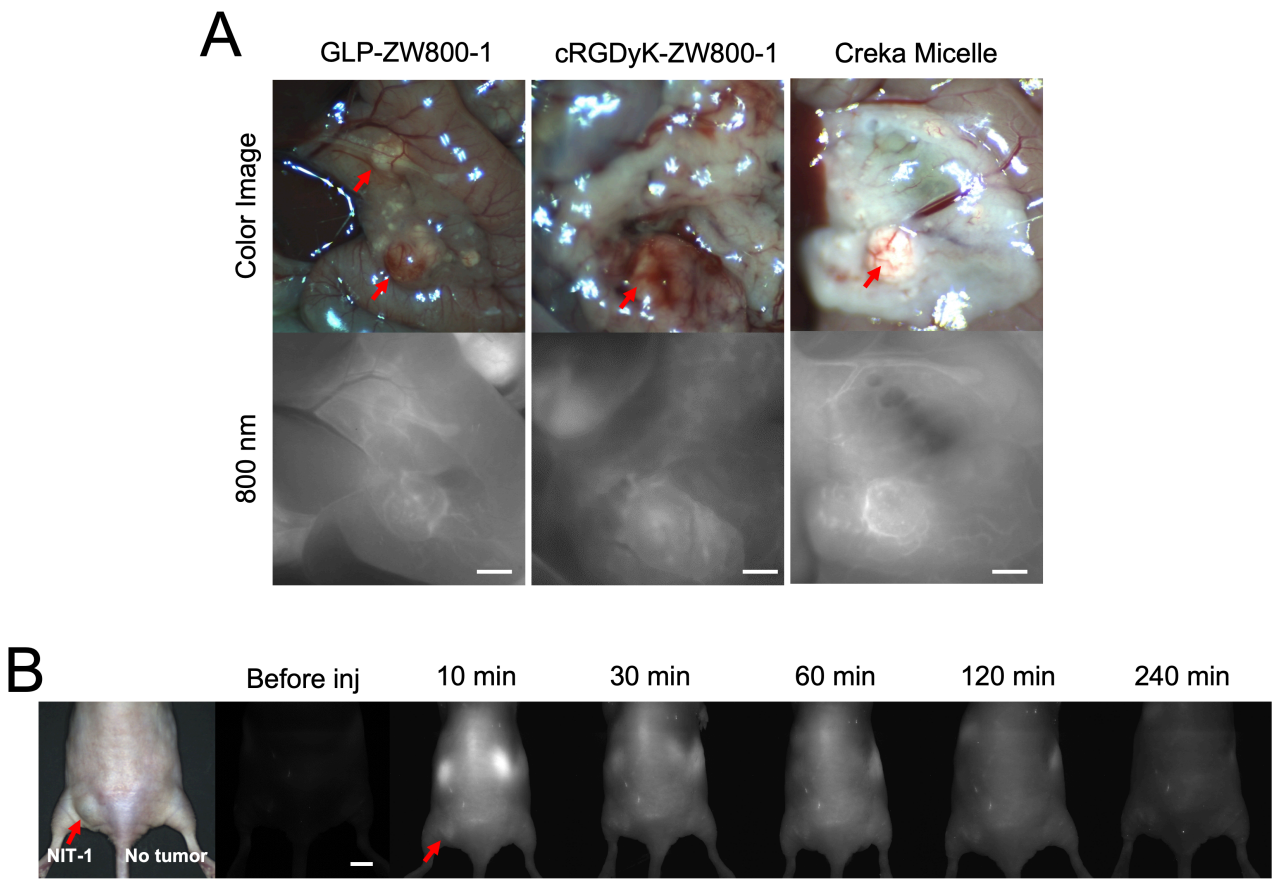

Figure S10. **Intraoperative tumor targeting using ZW800-1-conjugated peptides or proteins**, Related to Figure 4. **(A)** ZW800-1-conjugated GLP-1, cRGD or CREKA micelles were injected intravenously into insulinoma mice 1 h prior to imaging. Scale bars = 2 mm. **(B)** Nude mice with NIT-1 subcutaneous tumors were injected with 1.5 mg/kg of Ox61 and imaged up to 4 h. Scale bar = 5 mm.